Entanglement dynamics in a dispersively coupled qubit-oscillator system

D. Wahyu Utami and A. A. Clerk
Physics Department, McGill University, Montreal, Quebec, Canada H3A 2T8
(Received 12 March 2008; revised manuscript received 15 August 2008; published 23 October 2008)

We study entanglement dynamics in a system consisting of a qubit dispersively coupled to a finite-temperature, dissipative, driven oscillator. The robustness against dissipation of two generic kinds of entanglement is studied: the qubit can be entangled with either the phase or amplitude of the oscillator's motion. In the zero-temperature limit, an analytic expression is derived for the logarithmic negativity. We also discuss how the generated entanglement may be detected via dephasing revivals, being mindful that revivals can occur even in the absence of any useful entanglement.

DOI: 10.1103/PhysRevA.78.042323 PACS number(s): 03.67.Bg, 85.85.+j, 03.65.Yz

I. INTRODUCTION

There exists a long-standing interest in attempting to prepare and detect quantum states of macroscopic objects or collective degrees of freedom. Such an experiment would be more than a mere "proof of principle:" it would provide a nontrivial test of our understanding of the quantum dissipative processes which cause such states to degrade with time, and thus enforce the quantum to classical transition. Recent advances suggest that submicrometer-scale mechanical resonators could be excellent candidate systems in which to pursue this goal [1]. Such resonators contain a truly macroscopic number of atoms; at the same time, they can be fabricated to have high resonant frequencies and also high quality factors. This suggests that one has some hope of cooling these systems to close to their quantum ground state, and that decoherence due to the dissipative environment of the resonator should be slow—in standard models, decoherence rates scale with the oscillator damping rate [2]. Nanomechanical resonators also have the advantage that they can be strongly coupled to (possibly coherent) electronic degrees of freedom; this has recently been demonstrated to allow sensitive position detection, approaching the fundamental limits set by quantum back action [3–5].

In this paper, we analyze the entanglement dynamics in an electromechanical system where a dissipative mechanical resonator is dispersively coupled to a superconducting qubit: the state of the qubit simply shifts the frequency of the resonator [6,7]. Such a setup has the key advantage of being able to work with qubit states which are first-order insensitive to dephasing due to ever-present charge fluctuations [8,9]. As such, the system is substantially different from the one analyzed in the seminal proposal of Armour *et al.* [10], which made use of quickly dephasing superpositions of charge states in the qubit. While the dispersive coupling allows for longer qubit coherence times, there is a price to pay: unlike the proposal of Ref. [10], the two energy eigenstates of the qubit do not yield different average forces on the oscillator. As such, generating entanglement is a slightly more involved affair.

We demonstrate that, with a dispersive coupling, there are two generic ways to generate nonclassical, entangled oscillator-qubit states: one can entangle the qubit either with the *amplitude* of the oscillator's motion, or with its *phase*. We also study the robustness of these two kinds of entanglement against decoherence due to the dissipative environment, and discuss their detection using coherence revivals. A fully analytical expression for the entanglement (as measured by the logarithmic negativity) is obtained for the zero-temperature case. In the finite-temperature case, we make use of an exact solution of the master equation to efficiently calculate the time-dependent entanglement. We stress that the system studied here has already been realized in experiment, both with nanomechanical resonators [11], and with superconducting stripline resonators in circuit QED experiments [9]. Our study also sheds light on general questions of entanglement dynamics in the presence of dissipation, driving, and thermal noise, thus complementing other studies of entanglement in qubit-plus-oscillator models [12,13].

Note that issues of dispersive entanglement, while new in the context of quantum electromechanics, have been studied previously in atomic cavity QED systems. In particular, the groundbreaking experiment of Brune *et al.* [14] saw compelling evidence for entanglement between the state of an atom and the phase of a cavity coherent state. While theoretical work related to this experiment exists [15–17], our study differs in several key ways. We consider both phase and amplitude entanglement (as defined above), and are explicitly interested in the effects of finite temperature, something that is of crucial importance in nanomechanical systems. Unlike previous work, we also quantify the amount of entanglement using a rigorous entanglement monotone, the logarithmic negativity; we may thus rigorously distinguish a generic loss of qubit coherence from true qubit-oscillator entanglement.

II. SYSTEM

We consider a damped mechanical oscillator (frequency ω_M) which is dispersively coupled to a qubit (splitting frequency ω_{qb}). Setting $\hbar=1$, the Hamiltonian takes the form $H=H_0+H_\gamma$ with

$$H_0=(\omega_M+\lambda\hat{\sigma}_z)\left(\hat{a}^\dagger\hat{a}+\frac{1}{2}\right)+\frac{\omega_{\mathrm{qb}}}{2}\hat{\sigma}_z+f(t)(\hat{a}+\hat{a}^\dagger). \quad (1)$$

Here, λ is the strength of the dispersive coupling, $f(t)$ is a classical external force applied to the resonator, and H_γ de-

scribes the damping of the oscillator (damping rate γ) by an equilibrium Ohmic bath at temperature T. We stress that such a dispersive coupling can be easily realized in systems having nanomechanical resonators coupled to superconducting qubits, as it emerges naturally from a Jaynes-Cumming-type coupling in the relevant limit where $\omega_{\rm qb} \gg \omega_M$ [8]. Dispersive couplings have also been achieved in the same way in recent circuit QED experiments coupling superconducting qubits to stripline resonators [18].

The dispersive coupling implies that the two qubit energy eigenstates $|\uparrow\rangle, |\downarrow\rangle$ each lead to different oscillator frequencies; equivalently, the effective frequency of the qubit depends on the energy of the oscillator. Unlike previous proposals [10], the two qubit states do not yield different oscillator forces, making entanglement generation somewhat more subtle. One can easily show that if the oscillator starts in a thermal state and is not driven, then there is never any qubit-oscillator entanglement: the oscillator simply leads to a statistical uncertainty in the qubit's frequency. Entanglement generation thus necessarily requires that the oscillator start in a superposition of Fock states. The easiest experimental way to achieve this is by driving the resonator, resulting in a nonzero value of $\langle \hat{a}(t) \rangle$. We are thus led to consider entanglement in such (possibly) nonequilibrium states.

In what follows, we will focus on the experimentally relevant regime of a high Q factor resonator, and where $\lambda \ll \omega_M$. We may thus make use of the high-Q form of the Brownian-motion master equation for our system [7]:

$$\dot{\hat{\rho}} = -i[H_0, \hat{\rho}] + (\Gamma_\varphi/2)\mathcal{D}[\hat{\sigma}_z]\hat{\rho} + \gamma(n_{\rm eq}+1)\mathcal{D}[\hat{a}]\hat{\rho} + \gamma n_{\rm eq}\mathcal{D}[\hat{a}^\dagger]\rho, \tag{2}$$

where for any operator $\hat{A}$ we define

$$\mathcal{D}[\hat{A}]\hat{\rho} = \hat{A}\hat{\rho}\hat{A}^\dagger - (\hat{A}^\dagger\hat{A}\hat{\rho} + \hat{\rho}\hat{A}^\dagger\hat{A})/2. \tag{3}$$

Here, $\gamma \ll \omega_M$ is the damping rate of the resonator due the bath, and $n_{\rm eq}$ is a Bose-Einstein factor evaluated at the bath temperature T and energy ω_M. Γ_φ is the intrinsic dephasing rate of the qubit (i.e., dephasing due to sources other than the oscillator). We consider the usual situation where the qubit energy relaxation time is much longer than the dephasing time, and ignore T_1 processes.

We will further specialize to a class of experimentally relevant initial conditions where at $t=0$ there are no qubit-oscillator correlations. The qubit will be taken to be initially in the superposition state $|\psi\rangle = (|\uparrow\rangle + |\downarrow\rangle)/\sqrt{2}$, while the oscillator state will correspond to a thermal equilibrium state that has been displaced by the action of the classical driving force $f(t)$ (as yet unspecified). Such an uncorrelated state can be realized either by keeping the qubit-oscillator coupling off until $t=0$ (note that the coupling is tunable in electromechanical systems, e.g., Ref. [4]), or by quickly taking the qubit from its ground state $|\downarrow\rangle$ to $|\psi\rangle$ via a $\pi/2$ pulse. Note that each member in this class of initial states has a Gaussian form. As is discussed extensively in Ref. [7], Eq. (2) implies that such states remain Gaussian for all times, allowing an exact solution of their time evolution for arbitrary temperature and driving force. Full details of this calculation are provided in Ref. [7].

One can write the resulting solution for the qubit-oscillator density matrix in a physically transparent manner that is especially convenient for entanglement calculations. We first let $\hat{D}[\alpha]$ denote the displacement operator $\exp(\alpha\hat{a}^\dagger - \alpha^*\hat{a})$, $\sigma = \uparrow, \downarrow$ the two qubit states, and define

$$\hat{\rho}_{\sigma\sigma'} = {\rm Tr}_{\rm qb}(\hat{\rho}|\sigma'\rangle\langle\sigma|), \tag{4}$$

The solution for the qubit-diagonal parts of the density matrix may then be written as simple displaced thermal states:

$$\hat{\rho}_{\uparrow\uparrow}(t) = \tfrac{1}{2}\hat{D}[\alpha_\uparrow(t)]\hat{\rho}_{\rm eq}[T]\hat{D}^\dagger[\alpha_\uparrow(t)], \tag{5a}$$

$$\hat{\rho}_{\downarrow\downarrow}(t) = \tfrac{1}{2}\hat{D}[\alpha_\downarrow(t)]\hat{\rho}_{\rm eq}[T]\hat{D}^\dagger[\alpha_\downarrow(t)]. \tag{5b}$$

Here, $\hat{\rho}_{\rm eq}(T)$ is the thermal equilibrium oscillator density matrix at temperature T:

$$\hat{\rho}_{\rm eq}[T] = (1 - e^{-\Omega/(k_B T)})\sum_{n=0}^{\infty} e^{-n\Omega/(k_B T)}|n\rangle\langle n|. \tag{6}$$

Further, the displacement $\alpha_\sigma(t)$ is simply the mean value of $\hat{a}$ if the qubit state is frozen to be σ. $\alpha_\uparrow(t)$ and $\alpha_\downarrow(t)$ obey the expected classical equations of motion corresponding to a damped harmonic oscillator with frequency $\omega_M \pm \lambda$:

$$\alpha_\sigma(t) = {\rm Tr}(\hat{a}|\sigma\rangle\langle\sigma|\hat{\rho}(t)), \tag{7}$$

$$\dot{\alpha}_\sigma(t) = -i(\omega_M \pm \lambda - i\gamma/2)\alpha_\sigma(t) - if(t). \tag{8}$$

In contrast to the above, the solutions to the qubit-off-diagonal parts of the density matrix are more complex, and do not follow from some simple intuitive argument. We find

$$\hat{\rho}_{\uparrow\downarrow}(t) = [\hat{\rho}_{\downarrow\uparrow}(t)]^\dagger = \tfrac{1}{2}e^{i-\omega_{\rm qb}t}Y(t)\hat{D}[\tilde{\alpha}_\uparrow(t)] \times \{\hat{\rho}_{\rm eq}[T^*(t)]e^{-i\phi(t)(\hat{n}+1/2)}\}\hat{D}^\dagger[\tilde{\alpha}_\downarrow(t)]. \tag{9}$$

We see that $\hat{\rho}_{\uparrow\downarrow}$ also resembles a displaced thermal state. However, neither the temperature T^* nor the displacements $\tilde{\alpha}_\sigma$ are as expected: in fact, T^* is time dependent. In addition, there is an additional phase factor $\phi(t)$ resulting from the dependence of the qubit frequency on the resonator energy. Defining $\sigma(t) = \coth[(\omega_M/2T^*) + i\phi/2]$, one finds

$$\dot{\sigma} = -\gamma[\sigma - (2n_{\rm eq}+1)] - i\lambda(\sigma^2 - 1) \tag{10}$$

with the initial condition $T^*(0) = T$, $\phi(0) = 0$. In addition,

$$\tilde{\alpha}_{\uparrow/\downarrow} = (a_\pm) \pm (1 - {\rm Re}\,\sigma \mp i\,{\rm Im}\,\sigma)(a_+ - a_-)/(2\,{\rm Re}\,\sigma), \tag{11}$$

where we have defined

$$\dot{a}_\pm = [-i(\omega_M \pm \lambda\,{\rm Re}\,\sigma) - \tilde{\gamma}/2]a_\pm - if(t) \tag{12}$$

and $\tilde{\gamma} = \gamma + \lambda\omega_M\,{\rm Im}\,\sigma$. Note that the coherent state displacements $\tilde{\alpha}_\sigma$ coincide with the simple classical displacements α_σ only in the limit of zero temperature.

Finally, the prefactor $Y(t)$ in the expression for $\hat{\rho}_{\uparrow\downarrow}(t)$ in Eq. (9) describes the lack of purity of the qubit-oscillator

state: the qubit-oscillator system will in general not be in a pure state. This can result either from unwanted entanglement with the oscillator's dissipative bath, or from the intrinsic qubit dephasing described by Γ_φ in Eq. (2). Defining $p_n(T)=\langle n|\hat{\rho}_{\rm eq}(T)|n\rangle$ we find

$$Y(t)=\frac{e^{-\Gamma_\varphi t}\exp\left(-i\lambda\int_0^t dt'(\sigma+2a_+a_-^*)\right)}{\sum_n p_n(T^*)e^{-i\phi(n+1/2)}\langle n|\hat{D}^\dagger[\tilde{\alpha}_\downarrow]\hat{D}[\tilde{\alpha}_\uparrow]|n\rangle}. \quad (13)$$

III. ENTANGLEMENT

Having solved for the evolution of the density matrix in the previous section, we now turn to characterizing the amount of qubit-oscillator entanglement it possesses. This is somewhat involved, as in general our system will be in a mixed state. Similar to many recent works, we will use the logarithmic negativity E_N to quantify the amount of qubit-oscillator entanglement [19,20]. E_N is a rigorous entanglement monotone applicable to mixed state systems, and is strictly zero for unentangled systems. One has $E_N=\log_2(2\mathcal{N}+1)$, where the negativity $\mathcal{N}$ is the absolute value of the sum of the negative eigenvalues of the partially transposed density matrix $\hat{\rho}^{PT}$. It is worth emphasizing that the logarithmic negativity is a complex function of the *entire* density matrix, not just, e.g., the qubit coherence $\mathrm{Tr}\hat{\rho}_{\uparrow\downarrow}$. As such, even in the case of zero intrinsic qubit dephasing (i.e., $\Gamma_\varphi=0$), a loss of qubit coherence does not in itself imply the existence of any qubit-oscillator entanglement; such loss of coherence could instead be due to the effects of the oscillator's dissipative bath.

As discussed in the previous section, we always start from a state at $t=0$ where the qubit is uncorrelated with the oscillator, and is in an equal superposition of its two energy eigenstates. The two qubit states in this superposition each lead (via the dispersive coupling) to different oscillator frequencies; this difference will be exploited to yield entangled states which, in the absence of dissipation or thermal noise, would have the simple form

There are thus two generic ways to generate entanglement (see diagram in Fig. 1). The first is to entangle the qubit with the *phase* of the resonator, i.e., $\arg\langle\hat{a}\rangle$. The second generic approach is to entangle the qubit with the *amplitude* of the oscillator's motion, i.e., $|\langle\hat{a}\rangle|$. Note that entanglement with phase was studied in the seminal experiments of Brune *et al.* [14], and in related works of theory [15–17]. However, the logarithmic negativity associated with this kind of entanglement has not been studied before, nor its robustness against finite temperatures.

In what follows, we will discuss phase and amplitude entanglement at both zero and nonzero bath temperature T. In the zero-temperature case, the solution of the master equation in Eqs. (5) and (9) yields an exact expression for $E_N(t)$. Letting $\cos[\theta(t)]=|\langle\alpha_\uparrow(t)|\alpha_\downarrow(t)\rangle|$, one finds

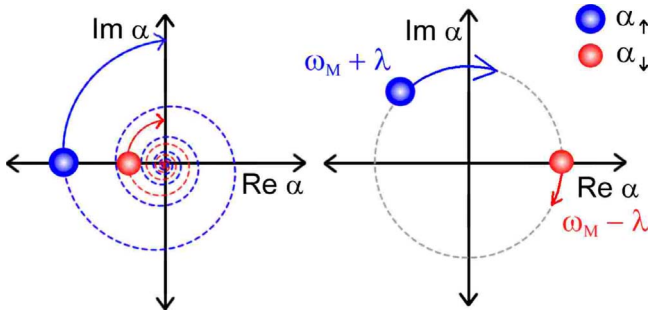

FIG. 1. (Color online) Illustration of amplitude entanglement (left) and phase entanglement (right). The two displaced states corresponding to the qubit up and down are drawn. In the case of amplitude entanglement, $\alpha_\uparrow$ gets driven to a higher oscillation amplitude compared to $\alpha_\downarrow$, as only $\alpha_\uparrow$ is on resonance. In the case of phase entanglement, there is no driving force; however, we start at a large coherent state amplitude. Both of the states gradually decay, but while this occurs, $\alpha_\uparrow$ oscillates faster than $\alpha_\downarrow$.

$$\mathcal{N}(t)=\frac{1}{4}[\sqrt{(1-|Y|)^2+4|Y|\sin^2\theta}-(1-|Y|)], \quad (15)$$

where for $T=0$ Eq. (13) for Y yields

$$|Y(t)|=\frac{e^{-\Gamma_\varphi t}\exp(-2\lambda\int_0^t dt'(|\alpha_\uparrow\alpha_\downarrow|\sin\phi_{\uparrow\downarrow}))}{\cos\theta(t)} \quad (16)$$

with $\phi_{\uparrow\downarrow}(t)=-\arg[\alpha_\uparrow(t)\alpha_\downarrow^*(t)]$. As expected, $\mathcal{N}$ (and hence the entanglement) is an increasing function of the distinguishability $\sin^2\theta$ of the two oscillator states. It is also a monotonically decreasing function of the purity $Y(t)$: as time progresses, the bath can distinguish the two oscillator states $|\alpha_\sigma\rangle$, thus reducing both $Y(t)$ and the amount of oscillator-qubit entanglement. One might expect that $|Y(t)|$ should depend only on the history of the overlap $\cos\theta(t')$; this is not the case. Instead, the decay of $|Y(t)|$ is sensitive to the history of $\sin\phi_{\uparrow\downarrow}(t)$, i.e., the sine of the relative phase between the two oscillator coherent state amplitudes. Somewhat surprisingly, times when $\phi_{\uparrow\downarrow}=\pi$ do not contribute to the decay of $|Y(t)|$, even though the overlap between the two oscillator coherent states is maximally small at such times.

Turning to the more general case where the bath temperature $T>0$, we again use our exact Eqs. (5)–(12) to solve for the system dynamics. Unfortunately, the resulting solution for the density matrix [as given in Eqs. (5)] does not allow for an exact evaluation of the logarithmic negativity. It does, however, allow for a simple numerical evaluation of $\mathcal{N}$: one simply converts $\hat{\rho}$ into a matrix in a basis of displaced Fock states, and then numerically finds the partial transpose and the corresponding negative eigenvalues. For $T>0$, $E_N(t)$ is not simply a function of the overlap $\langle\alpha_\uparrow|\alpha_\downarrow\rangle(t)$ and the purity $Y(t)$ [as given by the full expression Eq. (13)]—the entire matrix structure of $\hat{\rho}_{\uparrow\downarrow}$ is relevant.

Finally, in what follows we will be especially interested in how the oscillator dissipation affects the dynamics of entanglement. We will thus focus on the case of small intrinsic qubit dephasing, $\Gamma_\varphi\to 0$; we will comment on the effects of a nonzero Γ_φ in Sec. IV.

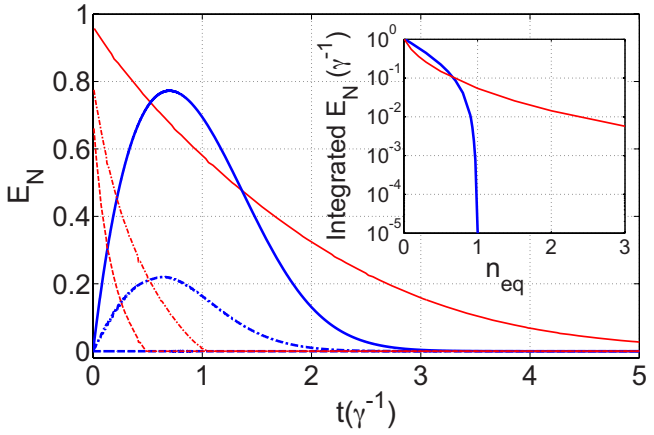

FIG. 2. (Color online) Logarithmic negativity E_N versus time. E_N is a non-monotonic function of time in the amplitude-entanglement setup, while it decays monotonically in the phase-entanglement setup. Blue lines correspond to the amplitude-entanglement setup; red lines correspond to the envelope of the oscillating E_N in the phase-entanglement setup. Solid lines are for $n_{\rm eq}=0$, dot-dashed for $n_{\rm eq}=0.5$, and dashed for $n_{\rm eq}=1.0$. For the phase-entanglement curves, we took $\alpha_0=0.76$ to maximize the total integral of $E_N(t)$ at $n_{\rm eq}=0$. We also chose $\alpha_f=3.74$ so that the integral of $E_N(t)$ for amplitude entanglement at $n_{\rm eq}=0$ is the same as the phase case. The inset shows the total time integral of E_N for both phase and amplitude entanglement as a function of $n_{\rm eq}$. In the phase-entanglement case, the integrated entanglement tends to zero near $n_{\rm eq}=1$. In all cases, $\lambda=0.01\omega_M$, $\gamma=10^{-5}\omega_M$, $\Gamma_\varphi=0$.

A. Amplitude entanglement

To entangle the qubit with the amplitude of the oscillator's motion, we start at $t=0$ with the qubit in a superposition of its eigenstates, and the oscillator in a thermal state with $\langle\hat{a}\rangle=0$. The oscillator is then driven with a force $f(t)=\gamma\alpha_f\cos[(\omega_M+\lambda)t]$ $(\alpha_f>0)$. In the relevant limit of a high-Q oscillator where $\gamma\ll\lambda$, $f(t)$ will cause $|\alpha_\uparrow(t)|$ to grow to a large value α_f, while $|\alpha_\downarrow|$ will be smaller by a large factor ω_M/γ: hence, the amplitude of the oscillator's motion will become entangled with state of the qubit, and we would expect the qubit-oscillator entanglement to grow with time. However, at long enough times, the dissipative bath coupled to the oscillator will destroy this entanglement: the bath can distinguish the two states $|\alpha_\sigma\rangle$, as described by $Y(t)$. These two competing tendencies lead to E_N being a nonmonotonic function of time; this is shown in Fig. 2.

At $T=0$, one can use Eqs. (5) and (15) to derive simple, exact expressions for $E_N(t)$ for the amplitude entanglement setup. Focusing on the relevant limit $\gamma\ll\lambda\ll\omega_M$, and taking $\Gamma_\varphi=0$, one finds that the negativity $\mathcal{N}(t)$ (and hence the entanglement) is independent of λ, and determined by

$$Y=\exp\left(\frac{(\alpha_f)^2}{2}[(2-e^{-\gamma t/2})^2-1-\gamma t]\right), \tag{17a}$$

$$\cos^2\theta=\exp[-(\alpha_f)^2(1-e^{-\gamma t/2})^2]. \tag{17b}$$

Note that in the long time limit the overlap $\cos\theta$ saturates, while $Y(t)$ decays exponentially to zero. This exponential decay is easily understood from Eq. (16): at long times, the phase difference $\phi_{\uparrow\downarrow}$ is nonzero and independent of time.

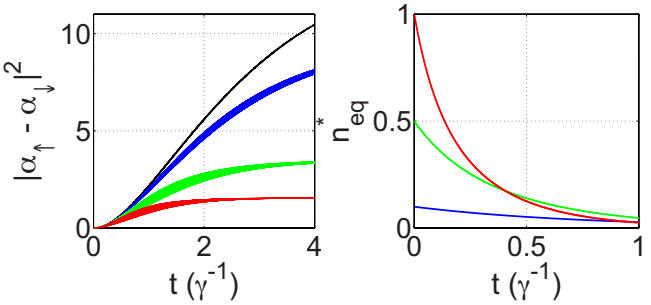

FIG. 3. (Color online) Left: Distance between effective oscillator displacements $\tilde{\alpha}_\uparrow(t)$, $\tilde{\alpha}_\downarrow(t)$ entering the expression for $\hat{\rho}_{\uparrow\downarrow}$. The apparent width of some curves is due to rapid oscillations with frequency λ/π. Right: Bose-Einstein factor associated with the effective temperature $T^*(t)$ appearing in the expression for $\hat{\rho}_{\uparrow\downarrow}$. Both cases are for the amplitude entanglement setup with $\alpha_f=3.74$. On the left, the highest curves correspond to the lowest $n_{\rm eq}=0$; on the right, the value of the curve at $t=0$ gives $n_{\rm eq}$. Temperatures are (black), 0.1 (blue), 0.5 (green), and 0.1 (red). λ, γ, and Γ_φ as in Fig. 1. For $T>0$, one finds $\tilde{\alpha}_\sigma\neq\alpha_\sigma$; temperature reduces the distinguishability of the $\tilde{\alpha}_\sigma$.

Nonzero temperatures dramatically suppress amplitude entanglement, as is shown in Fig. 2. Even though the two "classical" amplitudes $\alpha_\uparrow,\alpha_\downarrow$ continue to have very different magnitudes at $T>0$ (they are of course independent of T), the displacements $\tilde{\alpha}_\uparrow,\tilde{\alpha}_\downarrow$ which determine $\hat{\rho}_{\uparrow\downarrow}$ [cf. Eq. (9)] become less distinguishable as T is increased. This behavior is shown in Fig. 3, along with the time dependence of the effective temperature $T^*(t)$ appearing in the expression for $\hat{\rho}_{\uparrow\downarrow}$.

B. Phase entanglement

To entangle the qubit with the resonator phase, we prepare the system at $t=0$ so that the qubit is again in a superposition of its two eigenstates, and the oscillator is in a state of motion characterized by the coherent state amplitude α_0 (e.g., one could drive the oscillator at ω_m, keeping the coupling to the qubit off until $t=0$). All driving forces on the oscillator are turned off at $t=0$, and the coupled system is allowed to evolve. The magnitudes of both coherent states $\alpha_\uparrow,\alpha_\downarrow$ will be identical, and will decay at a rate γ. In contrast, the phase of the oscillator coherent state will wind at a frequency determined by the qubit. We have thus prepared a state where the phase, not the amplitude, of the oscillator's motion is entangled with the qubit.

Shown in the top panel of Fig. 4 is $E_N(t)$ for the phase entanglement setup, again in the case of zero intrinsic qubit dephasing. The entanglement drops to zero periodically at a frequency λ/π: at these times, the phases of the two oscillator states $\alpha_\uparrow,\alpha_\downarrow$ are aligned, implying $\cos\theta=1$. This alignment also implies that the coherence of the qubit is partially restored, as is shown in the bottom panel of Fig. 4, where we plot $2|\mathrm{Tr}\hat{\rho}_{\uparrow\downarrow}|$. These revivals of coherence are not perfect, as the dissipative bath leads the qubit-oscillator system to lose purity: one finds that the factor $Y(t)$ decays in a steplike fashion. This loss of purity also causes a gradually decaying

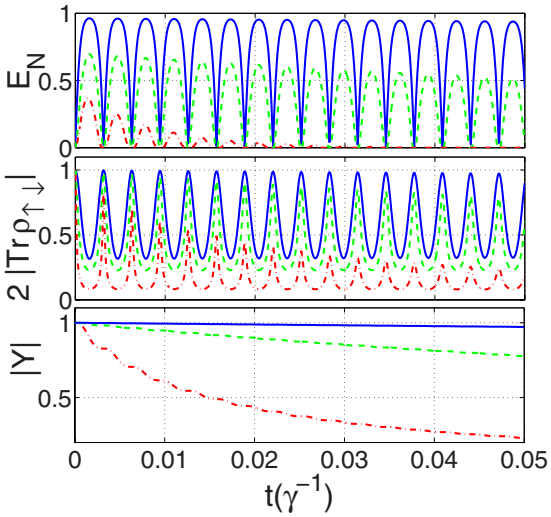

FIG. 4. (Color online) Phase entanglement. (a) Time-dependent logarithmic negativity E_N, $\alpha_0=0.76$. Solid line is for $n_{\rm eq}=0$, dashed for $n_{\rm eq}=1.0$, and dash-dotted for $n_{\rm eq}=5.0$. (b) Qubit recoherences associated with phase entanglement; same parameters. (c) Purity $|Y|$ of qubit-resonator system; same parameters. All with $\lambda, \gamma, \Gamma_\varphi$ as in Fig. 1.

envelope for the entanglement oscillations, as can be seen in Fig. 4. At zero temperature, and for $\gamma \ll \lambda \ll \omega_M$, the decay of $Y(t)$ is given by

$$Y(t) = \exp\left(-\frac{\alpha_0^2}{\gamma^2+4\lambda^2}\{4\lambda^2 - e^{-\gamma t}[4\lambda^2 + 2\gamma\lambda\sin(2\lambda t) + 2\gamma^2\sin^2(\lambda t)]\}\right). \quad (18)$$

Note that $Y(t)$ does not tend to zero in the long time limit.

It is interesting to note that for a fixed bath temperature the total amount of phase entanglement [as measured by the time integral of $E_N(t)$] has a maximum as a function of the initial coherent state amplitude α_0; this is shown in Fig. 5. For α_0 too small, the two oscillator states are not sufficiently distinguishable, and $E_N(t)=0$ remains small for all times, while for too large an α_0, the bath very rapidly distinguishes the two oscillator states in the superposition, and $E_N(t)$ decays rapidly to zero.

Finally, it is interesting to compare the phase and amplitude entanglement setups at finite temperature; this is done in Fig. 2, where we plot only the envelope of the oscillating entanglement in the phase case. As can be seen from the inset, phase entanglement is more robust against nonzero T than amplitude entanglement; the total time integral of $E_N(t)$ decays far more slowly as a function of $n_{\rm eq}$ in the phase case, for parameters that yield the same entanglement at $n_{\rm eq}=0$. Further, while both kinds of entanglement are suppressed by nonzero T, entanglement in the phase case can remain large for short times (i.e., for times t such that $1/\lambda \ll t \ll 1/\gamma$). Thus, phase entanglement shows a certain increased resilience against thermal dissipation compared to amplitude entanglement.

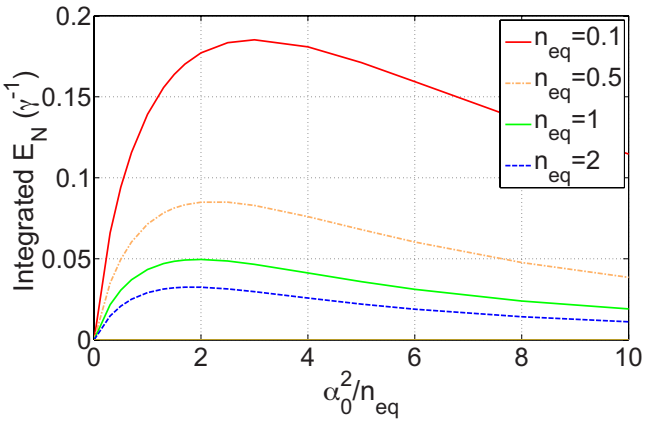

FIG. 5. (Color online) Total entanglement (as measured by the time integral of E_N) for the phase-entanglement setup, as a function of the initial coherent state amplitude α_0 and $n_{\rm eq}$. For a finite $n_{\rm eq}$, there is an optimal value of α_0 which maximizes the total entanglement. In all cases, $\lambda=0.01\omega_M$, $\gamma=10^{-5}\omega_M$, $\Gamma_\varphi=0$.

C. Detecting entanglement

We now discuss how entanglement may be detected using revivals in the coherence of the qubit. Consider the case of phase entanglement: as shown in Fig. 4, such entanglement leads to qubit recoherences [i.e., the magnitude of the qubit's off-diagonal density matrix element $|{\rm Tr}\hat{\rho}_{\uparrow\downarrow}(t)|$ is nonmonotonic in time]. This quantity represents the time-dependent dephasing of the qubit, and is measurable via either a standard Ramsey interference experiment [21], or via state tomography. While such revivals of coherence have been used to detect nonclassical states in other situations [22], and have been proposed as a way to detect entanglement in nanoelectromechanical system (NEMS) [10], one must be careful: it is possible to have coherence revivals without any qubit-oscillator entanglement. In our system, a purely thermal state oscillator state with $\langle\hat{a}(t)\rangle=0$ yields dephasing revivals, but zero qubit-oscillator entanglement.

Despite this caveat, one can still use dephasing revivals as a proxy for detecting entanglement. We focus on phase entanglement, as the amplitude-entanglement setup does not lead to any dephasing revivals, but rather a monotonic (but nonexponential) decay of $|{\rm Tr}\hat{\rho}_{\uparrow\downarrow}(t)|$. The basic idea in using coherence revivals to detect phase entanglement is that the Fourier spectrum of the time-dependent dephasing lets one unambiguously distinguish an initial thermal state with $\alpha=0$ and $E_N(t)=0$, from a phase-entangled state where $\alpha\neq 0$. This difference is essentially the number splitting effect discussed in Refs. [7,23,24], and measured in Ref. [18]: the peaks in the Fourier spectra are directly related to the number distribution in the oscillator. Thus, in a thermal state, one expects the peaks to follow a simple geometric series. In contrast, when α_0 is nonzero, the distribution begins to resemble more the Poisson distribution associated with a number state. Observing this difference, and comparing it to theory, would be a convincing way to detect the phase entanglement we have described. The difference between the two spectra is shown in Fig. 6.

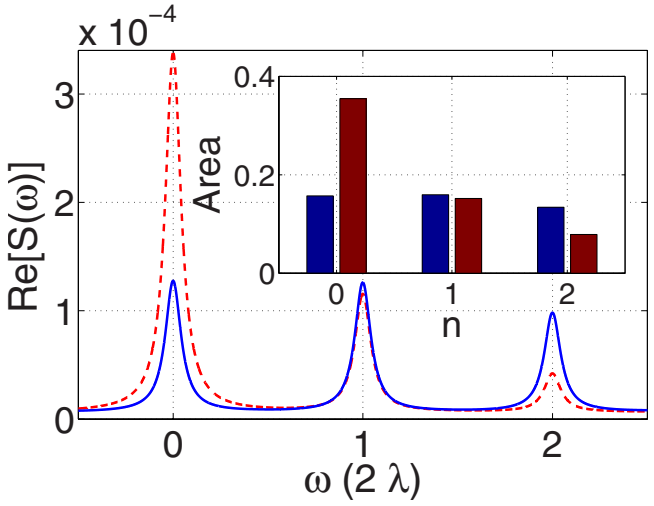

FIG. 6. (Color online) Phase-entanglement spectrum. $S(\omega)$, the real part of the Fourier transform of the qubit's time-dependent coherence $2|\mathrm{Tr}\hat{\rho}_{\uparrow\downarrow}(t)|$. The red dashed curve is for $n_{\mathrm{eq}}=0.5$, $\alpha_0=0$. There are revivals of coherence, but strictly zero qubit-oscillator entanglement; $S(\omega)$ shows peaks whose area follows a geometric series. In contrast, the solid blue curve corresponds to $\alpha_0=1.23$, $n_{\mathrm{eq}}=0.5$. Here, one gets both coherence revivals *and* entanglement. The dephasing spectrum is markedly different: the peak areas do not form a geometric series. The inset shows the integrated area for each spectrum in the two cases. All with $\lambda, \gamma, \Gamma_\varphi$ as in Fig. 1.

IV. EXPERIMENTAL CONSIDERATIONS AND CONCLUSIONS

To realize these ideas in a quantum electromechanical system, there are many challenges to be addressed. One must have a sufficiently strong qubit-resonator coupling. The resulting dispersive coupling λ must be much larger than both the resonator damping γ, as well as the intrinsic qubit dephasing rate Γ_φ. As indicated by Eq. (13), the qubit dephasing rate causes the purity $Y(t)$ of the qubit-oscillator state to decay over and above the decay causes by the oscillator's dissipative bath; this decay quickly causes a suppression of qubit-oscillator entanglement. In the case of phase entanglement, one would like to see several coherence revivals before this purity is lost: this requires λ larger than Γ_φ. While there are no published works on qubit-nanomechanical oscillators to date, work is actively under way [11]. In a related system, Naik *et al.* [4] were able to achieve a very strong coupling between a nanomechanical resonator and the central island of a superconducting single electron transistor. If this island had been used as a qubit, the corresponding dispersive coupling would have been $\lambda \sim 1$ MHz, much larger than the oscillator damping rate in the experiment, $\gamma \sim 200$ Hz. Further, state of the art experiments on superconducting qubits are able to achieve dephasing rates of $\Gamma_\varphi \sim 1$ MHz [25]. Thus, by combining these approaches, one is at least in striking distance of the parameters needed to realize the ideas discussed here.

A second key challenge for experiments is to achieve a low enough temperature that the effects of the dissipative bath are not too pronounced. The experiment of Ref. [4] was able to achieve $n_{\mathrm{eq}} \sim 25$; more recent experiments involving back-action cooling in NEMS are expected to achieve even lower oscillator temperatures. Our results are promising, as they show that even if the oscillator is not in its quantum ground state, one can still obtain appreciable entanglement.

In conclusion, we have studied entanglement in a dispersive qubit-oscillator system. We have identified two generic kinds of entanglement (phase and amplitude entanglement), and have shown that in general, phase entanglement is more robust against the effects of dissipation. We have also discussed how one can detect phase entanglement by using revivals in the qubit's coherence, and how one can distinguish this from revivals occurring without any qubit-oscillator entanglement.

ACKNOWLEDGMENTS

This work was supported by the Alfred P. Sloan Foundation, the Canadian Institute for Advanced Research, and NSERC.

[1] K. C. Schwab and M. L. Roukes, Phys. Today **58**(7), 36 (2005).
[2] J. P. Paz, S. Habib, and W. H. Zurek, Phys. Rev. D **47**, 488 (1993).
[3] R. G. Knobel and A. N. Cleland, Nature (London) **424**, 291 (2003).
[4] A. Naik, O. Buu, M. D. LaHaye, A. D. Armour, A. A. Clerk, M. P. Blencowe, and K. C. Schwab, Nature (London) **443**, 193 (2006).
[5] N. E. Flowers-Jacobs, D. R. Schmidt, and K. W. Lehnert, Phys. Rev. Lett. **98**, 096804 (2007).
[6] L. F. Wei, Y. X. Liu, C. P. Sun, and F. Nori, Phys. Rev. Lett. **97**, 237201 (2006).
[7] A. A. Clerk and D. W. Utami, Phys. Rev. A **75**, 042302 (2007).
[8] A. Blais, R.-S. Huang, A. Wallraff, S. M. Girvin, and R. J. Schoelkopf, Phys. Rev. A **69**, 062320 (2004).
[9] A. Wallraff, D. I. Schuster, A. Blais, L. Frunzio, R.-S. Huang, J. Majer, S. Kumar, S. M. Girvin, and R. J. Schoelkopf, Nature (London) **431**, 162 (2004).
[10] A. D. Armour, M. P. Blencowe, and K. C. Schwab, Phys. Rev. Lett. **88**, 148301 (2002).
[11] M. D. LaHaye and M. L. Roukes (private communication).
[12] T. A. Costi and R. H. McKenzie, Phys. Rev. A **68**, 034301 (2003).
[13] A. P. Hines, C. M. Dawson, R. H. McKenzie, and G. J. Milburn, Phys. Rev. A **70**, 022303 (2004).
[14] M. Brune, E. Hagley, J. Dreyer, X. Maitre, A. Maali, C. Wunderlich, J. M. Raimond, and S. Haroche, Phys. Rev. Lett. **77**, 4887 (1996).
[15] M. Brune, S. Haroche, J. M. Raimond, L. Davidovich, and N. Zagury, Phys. Rev. A **45**, 5193 (1992).

[16] J. G. Peixoto de Faria and M. C. Nemes, Phys. Rev. A **59**, 3918 (1999).
[17] J. M. Raimond, M. Brune, and S. Haroche, Rev. Mod. Phys. **73**, 565 (2001).
[18] D. Schuster *et al.*, Nature (London) **445**, 515 (2007).
[19] K. Zyczkowski, P. Horodecki, A. Sanpera, and M. Lewenstein, Phys. Rev. A **58**, 883 (1998).
[20] G. Vidal and R. F. Werner, Phys. Rev. A **65**, 032314 (2002).
[21] G. Ithier *et al.*, Phys. Rev. B **72**, 134519 (2005).
[22] T. Meunier, S. Gleyzes, P. Maioli, A. Auffeves, G. Nogues, M. Brune, J. M. Raimond, and S. Haroche, Phys. Rev. Lett. **94**, 010401 (2005).
[23] M. I. Dykman and M. A. Krivoglaz, Sov. Phys. Solid State **29**, 210 (1987).
[24] J. Gambetta, A. Blais, D. I. Schuster, A. Wallraff, L. Frunzio, J. Majer, M. H. Devoret, S. M. Girvin, and R. J. Schoelkopf, Phys. Rev. A **74**, 042318 (2006).
[25] J. A. Schreier *et al.*, Phys. Rev. B **77**, 180502(R) (2008).